Vegetable Research

ARTICLE

Open Access

https://doi.org/10.48130/vegres-0025-0004

Vegetable Research **2025**, 5: e009

Genome-wide identification of fasciclin-like arabinogalactan proteins (FLAs) in melon and the role of CmFLA8 in glucose accumulation in fruit

Suying Wen, Ruijie Huang, Muyao Gao, Jiayin Li, Yixuan Zhou, Rundi Sun, Zhilong Bie and Jintao Cheng*

National Key Laboratory for Germplasm Innovation & Utilization for Horticultural Crops, College of Horticulture and Forestry Sciences, Huazhong Agricultural University, Wuhan 430070, Hubei Province, China

* Corresponding author, E-mail: chengjintao@mail.hzau.edu.cn

Abstract

Fasciclin-like arabinogalactan proteins (FLAs) play an important role in plant growth and development. Nevertheless, little is known about FLA genes in melon. Here, we conducted a systematic analysis of the FLAs subfamily within the annotated genome of melon (*Cucumis melo* L.). Thirteen FLAs were identified, and with sequencing analysis categorized into four groups based on the presence of FAS domains and AGP-regions. Notably, five of the CmFLAs proteins contain a glycosylphosphatidylinositol anchor signal. Promoter *cis*-element prediction analysis indicated that the majority of the *CmFLAs* family members respond to abiotic stresses and hormones. The RNA-seq and qRT-PCR assays showed that *CmFLA10* exhibited specific expression patterns in male flowers, while *CmFLA12* was highly expressed in the root tissue. Notably, most of the *CmFLAs* genes were expressed at high levels during the early stages of fruit development, subsequently declining as the fruit ripened. Their expression levels were negatively correlated with the total soluble solids content. Treatment with β-Glc Yariv inhibited the expression of *CmFLA1*, *8*, *11*, and *13*, resulting in a significant increase in the sugar content of the fruits. Expression analysis suggested an induced up-regulation of genes associated with sugar metabolism. Subcellular localization studies demonstrated that CmFLA8 was localized in the cytoplasm. Overexpression of CmFLA8 in melon fruit resulted in a decrease in glucose content. In this study, *CmFLAs* play a negative role in sugar accumulation and fruit ripening in melon, providing new insights into FLA gene functions.

Citation: Wen S, Huang R, Gao M, Li J, Zhou Y, et al. 2025. Genome-wide identification of fasciclin-like arabinogalactan proteins (FLAs) in melon and the role of CmFLA8 in glucose accumulation in fruit. *Vegetable Research* 5: e009 https://doi.org/10.48130/vegres-0025-0004

Introduction

Hydroxyproline-rich glycoproteins (HRGPs) comprise a major group of structural proteins in the plant cell walls and are essential for plant growth and development[1,2]. The arabinogalactan proteins (AGPs), a subfamily of HRGPs, are highly glycosylated glycoproteins found in the plasma membranes, cell walls, extracellular spaces, and in secretions (e.g., stigma surface)[3]. The β-glucosyl Yariv reagent (β-Glc Yariv) and anti-AGP monoclonal antibodies can specifically interact with AGPs and are used to clarify their functions[4]. β-Glc Yariv binds AGPs through β-1,3-galactan chains[5]. In plants, AGPs participate in fruit ripening[6,7]. Typically, classic AGPs contain three characteristic domains: N-terminal secretion signal, Pro/Hyp-rich domain, and a C-terminal glycosylphosphatidylinositol (GPI) plasma member anchor. Classical AGPs include the Lys-rich classical AGPs, arabinogalactan (AG) peptides, and chimeric AGPs[1].

Fasciclin-like arabinogalactan proteins (FLAs) are classified as chimeric AGPs. Apart from one or two AGP motifs, FLAs possess one or two specific fasciclin (FAS) domains containing conserved regions H1 and H2 regions and contribute to cell adhesion and communication[1,8–11]. Structural analysis of AtFLA4 revealed that the FAS1 domain is required to stabilize plasma membrane localization, while the GPI-modification signal facilitates membrane attachment and endoplasmic reticulum (ER)-exit; N-glycosylated acts for ER-exit, while O-glycosylation affects post-secretory fate[12].

Numerous *FLA* genes have been identified across various plant species, with examples including 21, 27, 34, and 19 FLAs in Arabidopsis (*Arabidopsis thaliana*), rice (*Oryza sativa*), wheat (*Triticum aestivum*), cotton (*Gossypium hirsutum*), respectively[1,10,11,13,14]. FLAs play crucial roles in plant growth and development, such as fiber development[4,15–17], sexual reproduction[18–20], cell wall regeneration[21], and responsiveness to environmental conditions[22–24]. Notably, FLA genes have been extensively investigated in Arabidopsis. For instance, AtFLA18 regulates root elongation[25]; AtFLA12 and 16 contribute to stem development and differentiation[26,27]. Additionally, AtFLA3 and AtFLA14 are specifically expressed in pollen grains, playing an essential role in pollen development[18,28]. Ceitain *FLA* genes respond to stresses and plant hormones. For instance, *FLA4*, also known as *salt overly sensitive 5* (*SOS5*), is sensitive to salt stress and affects cell-to-cell adhesion[29]. This gene acts within a linear pathway alongside FEI1/2, the leucine-rich repeat receptor-like kinases (RLKs), to modulate cell expansion dependent on ACC-mediated signals[30]. Drought leads to reduced expression of *FLA9*, and increases seed abortion in maize and Arabidopsis[23]. Consequently, FLAs are likely to play pivotal roles in plant growth and development. However, the exact underlying mechanism remains unclear.

Melon (*Cucumis melo* L.) is a vital commercial horticultural crop worldwide, belonging to the *Cucurbitaceae* family. Melon cultivars exhibit diversity, their fruit vary in size, shape, fresh color, rind color, texture, aroma, flavor, and nutritional value[31]. The function of *FLAs* in melon remains uncertain. Therefore, comprehensive bioinformatics analysis and identification of *FLAs* should be conducted within the melon genome.

In the present study, we identified 13 putative *FLA* genes in the melon genome and conducted a comprehensive analysis of *CmFLAs* using a bioinformatics approach. This analysis contained gene structure, motifs, physiochemical properties, domain analysis, chromosomal localization, subcellular localization, and phylogenetic comparison with other species. Additionally, we determined the expression patterns of these *FLAs* using publicly available RNA-seq data. Subsequently, we conducted qRT-PCR analysis to validate the expression

of *CmFLAs* in melon fruits and to investigate their response to ABA signaling pathways. Finally, we further investigated the function of CmFLA8 in the regulation of sugar accumulation in melon fruit. This study offers fundamental insights into *CmFLAs* and may expedite the functional analysis of *FLA* genes in melon.

Materials and methods

Identification of *CmFLA* genes in melon

All the sequence data of *Cucumis melo* L. cv. DHL92 (.fasta files) was downloaded from the cucurbit genomics database (http://cucurbitgenomics.org). Proteins containing FAS domains were identified using several prediction algorithms (http://pfam.sanger.uk, PF02469, http://smart.embl-heidelberg.de, SM00554, and www.ebi.ac.uk/interpro, IPR000782). Subsequently, the N-terminal signal sequences of these proteins were assessed using SignalP 5.0 (www.cbs.dtu.dk/services/SignalP)[32]. The presence of C-terminal GPI-addition signals was predicted using the big-PI Plant Predictor (https://mendel.imp.ac.at/gpi/plant_server.html)[33]. After filtering out proteins without N-terminal sequences, the remaining proteins with FAS domains were manually inspected for potential AGP-regions. Ultimately, proteins containing both FAS domains and AGP-like glycosylated regions were considered as CmFLA. The proportions of Pro, Ala, Ser, and Thr (PAST) are the putative CmFLAs were calculated using a Perl script[1].

We utilized ExPASy (https://web.expasy.org/protparam) to analyze the physical and chemical parameters of proteins[34]. The subcellular localization of CmFLAs was determined using WoLF PSORT (www.genscript.com/tools/wolf-psort)[35]. *N*-glycosylation and *O*-glycosylation of the putative FLAs were investigated using NetNGlyc (www.cbs.dtu.dk/services/NetNGlyc)[36] and NetOGlyc (www.cbs.dtu.dk/services/NetOGlyc)[37]. Additionally, GO annotation of *CmFLAs*, describing biological processes, cellular components, and molecular functions, was obtained from the cucurbit genomics database (http://cucurbitgenomics.org).

Chromosomal localization and gene structure analysis

All of the gene information (gff3 files) was downloaded from cucurbit genomics (http://cucurbitgenomics.org). The chromosomal distribution of *CmFLA* genes was established using the positions of *CmFLA* genes from the melon database and visualized using TBtools software[38]. Furthermore, the conserved motifs of these genes were examined using NCBI Batch CD-Search[39] and the MEME program (https://meme.nbcr.net/meme)[40]. The CDS and gene structure were also determined using TBtools software[38].

Alignment and phylogenetic analysis

The fasciclin-like domain sequences of CmFLAs were generated using ClustalX (2.1) and were manually corrected[41]. A phylogenetic tree was constructed using the neighbor-joining method in MEGA7 software[42] and EvolView version 2 (www.evolgenius.info/evolview-v2)[43], with a bootstrap value of 1,000.

Plant material and growth conditions

Various varieties of melon plants (*Cucumis melo* L., including cv. Balengcui (BLC), cv. Baicaigua (BCG), cv. Huapicaigua (HPC), cv. Xiaomaisu (XM), cv. Yangjiaosu (YJ), cv. Longtian No.4 (LT4), cv. Gaoshicui (GS), cv. M43) were grown in polytunnels in Wuhan, China, from March to June. Melon fruits were harvested 30 d after anthesis (DAA) for qRT-PCR and sugar quantification. All fruit samples were promptly frozen in liquid nitrogen and stored at −80 °C before usage.

RNA-seq analysis

RNA-seq data from the database of cucurbit genomics (https://cucurbitgenomics.org/) were analyzed. PRJNA383830, which contains samples from diverse tissues of melon, and PRJNA286120, covering different developmental phases of green and orange fruit flesh, were used for analysis. The heatmap was created using TBtools software[38].

Cis-acting elements analysis

The 2 kb upstream region of each CmFLA gene was extracted as the promoter region, and the potential *cis*-elements were analyzed in PlantCARE database (https://bioinformatics.psb.ugent.be/webtools/plantcare/html)[44]. The diagrams were generated using the TBtools software[38].

Total soluble solids content (TSS) evaluation

The TSS of each melon fruit was measured by dropping the extracted juice from the equatorial region of flesh tissue onto a digital refractometer. The value reported for each sample represents the average of three replicates.

ABA treatment

Melon fruit of the cv. 'Boyang' at 20 DAA were chosen for ABA treatment, the fruit discs were immersed in a solution of 100 μM ABA, with water used as the control. The discs were shaken at 25 °C for 8 h, with each treatment having three biological replicates. Following three washes with water, the samples were prepared for further analysis.

β-Glc Yariv treatment

Melon fruits of the cv. 'BCG' at 20 DAA were sprayed with a solution containing 200 mg/L β-Glc Yariv (Biosupplies, Australia), with water used as the control. Each treatment involved three fruits. Fruit samples were collected from the plants after 5 d of treatments for further analysis.

Sugar content measurements

Fruit samples, which were collected and stored at −80 °C, were ground to powder using liquid nitrogen. It was used for measuring the sucrose, fructose, and glucose content by gas chromatography (GC), following the method by Cheng et al.[45]. The ground samples (1 to 2 g) were extracted by ultrasonication in an extraction solution containing 80% ice-cold methanol and 0.1 M imidazole at 70 °C for 30 min. Subsequently, the mixture was centrifuged at 4,000 × g for 30 min. The supernatant was mixed with an internal standard (methyl-a-D-glucopyranoside, Sigma, USA) and was dried using Speed Vac (Eppendorf, Germany) at 45 °C for 2 h. The dried samples were derivatized using hydroxylamine hydrochloride: hexamethyldisilazane: trimethylchlorosilane before analysis by GC (Agilent 7890B).

Standard solutions of fructose, glucose, and sucrose (Sigma, USA) were prepared. Subsequently, standard curves and correlation coefficients were obtained as described above. Thus, we calculated the sugar content of the samples from standard curves.

RNA extraction and cDNA synthesis

Total RNA was extracted from melon fruits at 30 DAA using TRIzol. One μg of total RNA was utilized for cDNA synthesis with HighScript III reverse transcriptase after genomic DNA removal.

qRT-PCR analysis

The cDNA served as the template for qRT-PCR analysis, conducted on the ABI7500 system (Bio-Rad) using the SYBR green detection protocol (TaKaRa). TUA (α-tubulin) was used as a reference gene. Primers used for qRT-PCR analysis can be found in Supplementary Table S1. Finally, the mean expression level of relevant genes was calculated using the $2^{-\Delta\Delta CT}$ method[46].

Subcellular localization

To determine the subcellular localization of CmFLA8, firstly, we used the primers (F: 5'-ATGGCGCCTTCCAAATCTC-3'; R: 5'-TTAGGACA ATAAAAGGGAGG-3') to clone the CDS of *CmFLA8*. Then, the full-length CDS of *CmFLA8* without a stop codon was inserted into pH7LIC6.0-ccdB rc-C-eGFP. The vector was linearized by *Stu* I and assembled through Gibson one-step assembly method. Subsequently, a transient expression method using *A. tumefaciens* (strain GV3101) was employed to introduce the vector into *N. benthamiana* leaves[45]. The resulting fluorescence was visualized using a confocal microscope (Leica SP8). GFP was excited with 488 nm, and fluorescence emissions of 495 to 531 nm were collected. Chloroplasts autofluorescence was excited with 552 nm, and fluorescence emissions between 644 and 697 nm were collected.

Agrobacterium-mediated transient transformation

For the overexpression of CmFLA8 in cv. 'XM' melon fruit, the full-length CDS of *CmFLA8* was cloned into the pHELLSGATE8-HA vector. The vector was linearized by *Eco*R I and *Kpn* I, then assembled through Gibson one-step assembly method. Subsequently, the resulting recombinant plasmids were introduced into *A. tumefaciens* (strain GV3101). The cultures were then resuspended in an infiltration buffer containing 50 mM MES, pH 5.6, 10 mM $MgCl_2$, and 1 mM acetosyringone, reaching an OD_{600} cell density of 0.3–0.4. This infiltration buffer was then injected into cv. 'XM' melon fruit at 15–20 DAA to a depth of 0.5 cm. An empty vector served as the control. Each fruit underwent three injections, and each treatment was administered to four fruits. The infiltrated fruit was harvested 5 d post-injection, and the fruit flesh surrounding the infiltrated area was sampled for subsequent analysis.

Results

Identification of putative FLA genes in the melon genome

A Perl script (amino acid bias) can hardly locate FLAs based on the low proportions of PAST residues[13]. Therefore, we utilized the hidden Markov model (multiple sequence alignments), as described by Schultz et al.[47], to detect proteins with low similarity. Subsequent searches in the Pfam (PF02469), SMART (SM00554), and InterPro (IPR000782) databases, 19 predicted melon proteins containing FAS domains were found. Among these, three genes (MELO3C008283.2, MELO3C005314.2, and MELO3C018783.2) were excluded using SignalP5.0 due to the absence of N-terminal signal peptides. We manually examined the presence of AGP regions. According to Schultz et al.[47], non-contiguous Hyp residues with no more than 11 amino acid residues between consecutive Hyp residues (e.g., [A/S/T]-P-X(0,10)–[A/S/T]-P) are likely to be galactosylated[11,47]. Additionally, contiguous Hyp residues, such as [A/S/T]-P-P and [A/S/T]-P-P-P, indicated arabinosylated[48,49]. Ultimately, 13 putative *CmFLAs* contained these glycomodules, with the exception of three *CmFLAs* genes: MELO3C024107.2, MELO3C028604.2, and MELO3C012299.2.

Detailed information about the 13 putative CmFLAs is presented in Table 1. The amino acid sequences consist of 243–466 amino acids, with each FLA containing one or two FAS domains and one or two AGP regions. Among the CmFLAs, five FLAs (CmFLA1, 2, 6, 8, and 9) possess a GPI anchor signal. All CmFLAs exhibit N-terminal secretion signals, with the possible cleavage sites specified in Table 1.

The chromosome distribution of *CmFLA* genes in *Cucumis melo* L. was investigated. These genes were distributed on seven chromosomes in the melon genome, with four genes (*CmFLA1, 2, 6,* and *7*) located on chromosome 01 (Fig. 1a). Additionally, the amino acid sequences of these proteins were aligned, and a phylogenetic tree was constructed (Fig. 1b). These genes were categorized into three clades: Clade I includes CmFLA1, 2, 5, 7, 8, 9, and 12; CmFLA6, 11, and 13 were clustered into Clade II; and Clade III comprises CmFLA3, 4, and 10 (Fig. 1b).

The characteristic regions of CmFLAs were investigated via conserved motif prediction, leading to the identification of 13 motifs in melon FLA proteins (Fig. 1c; Supplementary Table S2). Motifs 1 and 2 were found in all CmFLAs, indicating their significance for FLA proteins. Moreover, motifs 3, 4, and 7 were present in most CmFLAs, indicating their necessity for FLA. Conversely, motifs 8, 9, 10, 12, and 13 were exclusive to CmFLA3 and CmFLA4, suggesting distinct functions compared to other CmFLAs. Notably, five CmFLAs (CmFLA5, 6, 7, 11, and 13) shared identical conserved motifs, implying similar function (Fig. 1c). Furthermore, *CmFLA1*, *5*, *8*, *10*, *11*, and *12* contained one exon, *CmFLA3, 4, 6, 7, 9*, and *13* included two exons, while *CmFLA2* had three exons (Fig. 1d).

Characteristics of CmFLA proteins

CmFLAs were further characterized through an analysis of their molecular weight (MW), pI, GRAVY index, PAST content, putative *O*-glycosylation sites, putative *N*-glycosylation sites, and subcellular localization. The data are summarized in Table 2. The MW of CmFLA proteins ranged from 25.81 to 51.48 kD, while the pI value is within the range of 4.23 to 6.18. Among the CmFLAs, CmFLA2, CmFLA3, CmFLA4, CmFLA10, and CmFLA13 were identified as hydrophilic proteins, whereas the rest exhibited hydrophobic proteins.

Table 1. Putative *FLA* genes identified in the genome of *Cucumis melo*. L.

Protein name	Gene ID	Chromosome location	Strand	Size (aa)	FASs	AGPs	GPI	SP	Possible cleavage site
CmFLA1	*MELO3C024938.2*	Chr01: 10881922, 10883631	–	414	1	2	Y	Y	28~29
CmFLA2	*MELO3C024192.2*	Chr01: 4351699, 4354505	+	421	2	2	Y	Y	30~31
CmFLA3	*MELO3C015093.2*	Chr02: 8392291, 8395918	+	466	2	2	N	Y	26~27
CmFLA4	*MELO3C009567.2*	Chr04: 31139948, 31143044	+	465	2	1	N	Y	26~27
CmFLA5	*MELO3C019361.2*	Chr11: 12828056, 12829226	–	263	1	2	N	Y	23~24
CmFLA6	*MELO3C018862.2*	Chr01: 3459779, 3461694	+	247	1	2	Y	Y	18~19
CmFLA7	*MELO3C018888.2*	Chr01: 3762092, 3763889	–	255	1	2	N	Y	23~24
CmFLA8	*MELO3C022507.2*	Chr11: 34215140, 34216937	–	423	1	2	Y	Y	18~19
CmFLA9	*MELO3C020643.2*	Chr12: 1931250, 1932848	+	352	1	1	Y	Y	26~27
CmFLA10	*MELO3C014385.2*	Chr05: 2950327, 2951358	+	343	1	1	N	Y	32~33
CmFLA11	*MELO3C014248.2*	Chr05: 4832311, 4833298	–	248	1	1	N	Y	23~24
CmFLA12	*MELO3C014107.2*	Chr06: 36961275, 36962122	+	248	1	2	N	Y	18~19
CmFLA13	*MELO3C005051.2*	Chr12: 3927483, 3929729	+	243	1	2	N	Y	22~23

SP: Signal Peptide; aa: amino acid.

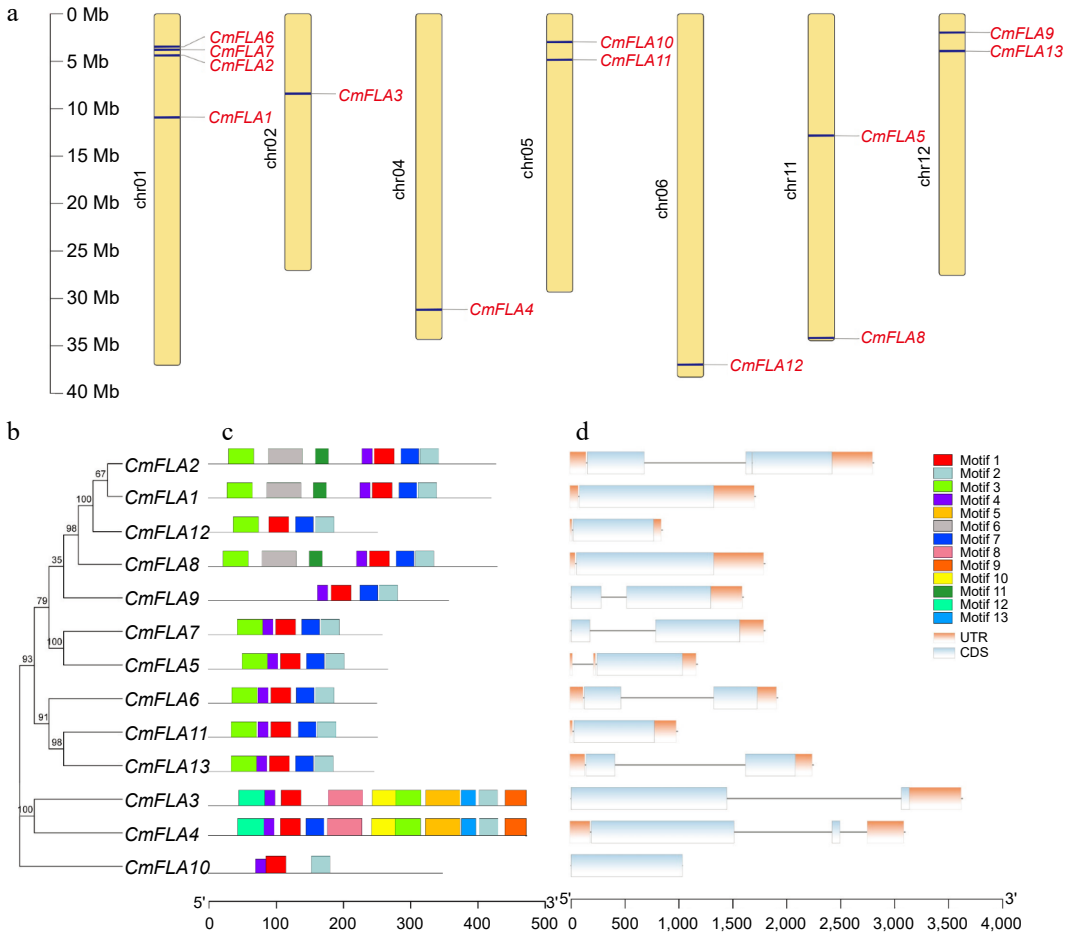

Fig. 1 Gene location, conserved motif, and gene structure analysis of CmFLAs. (a) Distribution of *CmFLA* genes on melon chromosomes. Thirteen genes were mapped to 7 out of 12 chromosomes. The dark blue lines represent the gene positions on the chromosome. The dark line in the left panel represents the chromosome scale. (b) The phylogenetic relationship among *CmFLAs*. (c) Conserved motif analysis of *CmFLAs*. Thirteen predicted motifs are represented by different colored boxes. The sequence information for each motif is provided in Supplementary Table S2. (d) Gene structure analysis of *CmFLAs*. Exons are denoted by light blue boxes, UTRs by orange boxes, and introns by gray lines.

Table 2. Characteristics of FLA proteins in melon.

Protein name	MW (kDa)	pI	GRAVY	PAST	Number of *N*-glycosylation	Number of *O*-glycosylation	Predicated subcellular localization
CmFLA1	44.15	5.88	0.013	32.6%	6	14	Chloroplast
CmFLA2	45.02	5.45	−0.011	31.5%	5	14	Chloroplast
CmFLA3	51.48	6.18	−0.312	29.4%	2	15	Vacuolar
CmFLA4	51.13	6.03	−0.287	29.4%	2	20	Chloroplast
CmFLA5	27.92	5.57	0.197	38.4%	3	16	Cytoplasmic
CmFLA6	25.81	5.62	0.071	33.6%	4	5	Chloroplast
CmFLA7	26.91	5.32	0.139	40.0%	4	14	Plasma membrane
CmFLA8	43.32	5.63	0.218	43.4%	5	35	Plasma membrane
CmFLA9	37.47	5.06	0.319	33.0%	5	11	Extracellular
CmFLA10	37.41	5.83	−0.041	38.5%	2	25	Chloroplast
CmFLA11	25.94	5.14	0.028	35.6%	4	16	Chloroplast
CmFLA12	26.27	4.23	0.087	34.8%	1	15	Chloroplast
CmFLA13	26.05	4.73	−0.040	33.0%	4	6	Extracellular

Notably, the proportion of PAST residues in CmFLAs ranged from 29.4% to 43.4%. All CmFLAs harbored putative *N*-glycosylation sites and putative *O*-glycosylation sites (Table 2). Subsequent analysis of putative subcellular localization revealed distinct patterns: CmFLA1, 2, 4, 6, 10, 11, and 12 were localized in the chloroplast, CmFLA9 and 13 in the extracellular domain, CmFLA7 and 8 in the plasma membrane, CmFLA3 in the vacuolar, and CmFLA5 on the cytoplasmic membrane (Table 2).

Protein structure and phylogenetic analysis

FAS domains consist of 110–150 amino acids and exhibit low sequence similarity[10]. Putative FAS domains within CmFLA proteins were aligned using the ClustalX program, revealing conserved regions depicted in the smart00554 motif, namely, the H1 and H2 conserved region, and the [Tyr Phe] His ([YF]H) motif situated between H1 and H2 regions. The Thr residue within the H1 region is

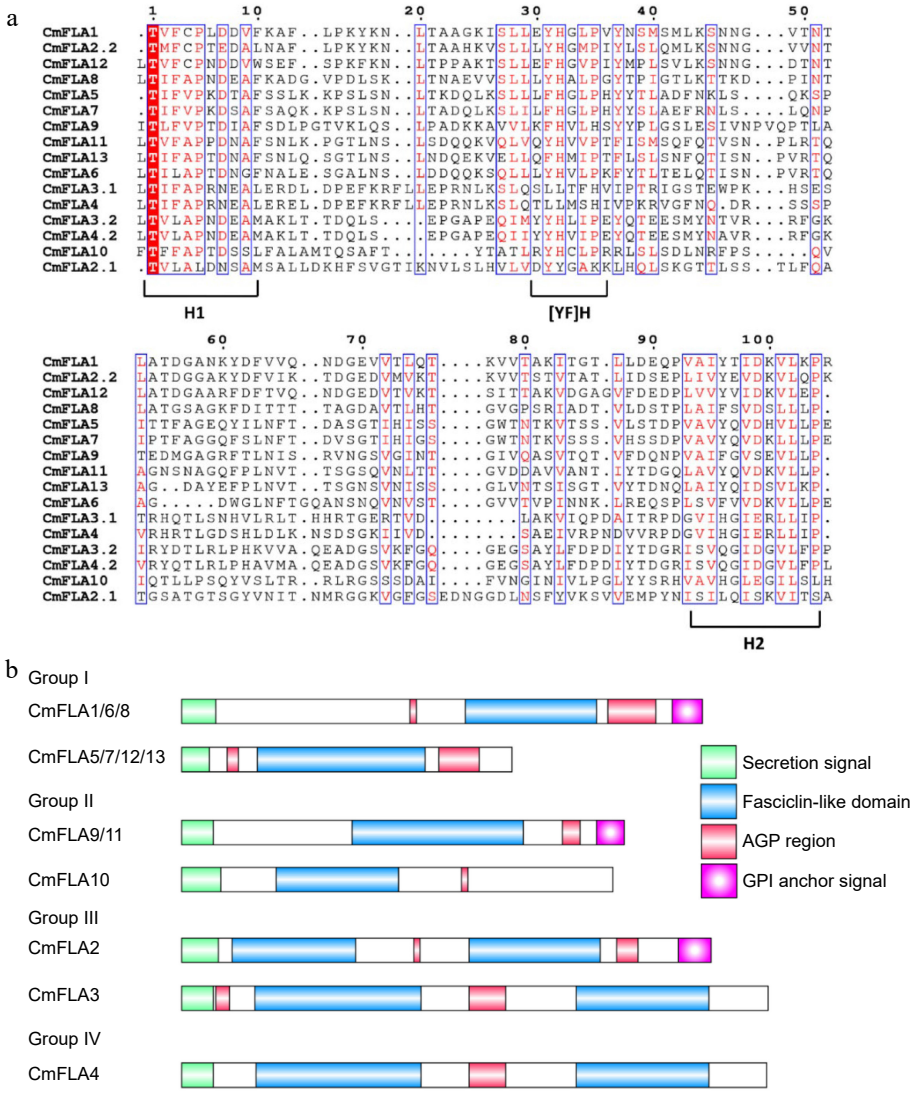

Fig. 2 Domain analysis of CmFLAs. (a) Multiple sequences alignment of the CmFLA FAS domains. Two FAS domains present in the protein. The domain closest to the N-terminus is indicated by .1, followed by .2. (b) Schematic representation of the CmFLAs deduced from DNA sequence. The FLAs are grouped into four (I–IV) based on the numbers of AGP-like regions and FAS domains. The indicated regions include the signal peptide (green), FAS-like domains (blue), AGP domain (red), and GPI-anchoring signal (purple box with a white point inside).

completely conserved in the FAS -like domain[11]. All FAS domains of CmFLAs contained these conserved regions (Fig. 2a).

Considering the numbers of AGP-like regions and FAS domains as described by Xu et al.[30] with modification, these CmFLAs could be divided into four groups (Fig. 2b). Group I consisted of members with one FAS domain and two AGP regions, including CmFLA1, 5, 6, 7, 8, 12, and 13, while CmFLA9, 10, and 11 belonged to Group II, where one FAS domain was flanked by one AGP-like glycosylated region. Group III comprised CmFLA2 and CmFLA3, each containing two FAS domains and two AGP glycosylated regions. Finally, CmFLA4 was categorized into Group IV, characterized by two FAS domains with one AGP glycosylated region.

A comparison of the FLA protein homoeologous between Arabidopsis and melon reveals the amino acid identities of CmFLAs and AtFLAs, are detailed in Supplementary Table S3. The amino acid identity between AtFLA16 and CmFLA4 was 77.49%, while that between AtFLA16 and CmFLA3 was 79%. Two members exhibit high sequence homology with AtFLA7, namely CmFLA5 (71.71%) and CmFLA7 (77.33%, Supplementary Table S3). To explore the evolutionary relationships among the FLA genes of different species, a phylogenetic tree was constructed using the full-length sequence of 13 CmFLAs, 21 AtFLAs, 27 OsFLAs, and 19 GhFLAs (Fig. 3). These FLAs were divided into nine classes. Notably, CmFLA1, CmFLA2, AtFLA1, AtFLA3, and AtFLA14 belong to the same class. Additionally, CmFLA11, CmFLA13, AtFLA11, AtFLA12, and GhFLA1 are evolutionally close (Fig. 3).

Expression analysis of *CmFLAs* genes in various organs and fruit at different developmental stages

The expression patterns of *CmFLAs* genes in different organs of melon were revealed using the public RNA-seq resource in the cucurbit genomic database. It was observed that all *CmFLAs* showed low expression level in mature fruit (Fig. 4a). *CmFLA10* was specifically expressed in male flower, while *CmFLA12* showed abundant expression in the root. Interestingly, three genes (*CmFLA6*, *CmFLA11*, and *CmFLA13*) displayed a similar expression pattern across different tissues, with high expression levels in both the root and leaf.

To further investigate the gene expression during different development periods of the fruit, we utilized additional RNA-seq data collected from two cultivars of melon. The expression patterns of *CmFLA10* were observed to be low in both two cultivars. *CmFLA12*

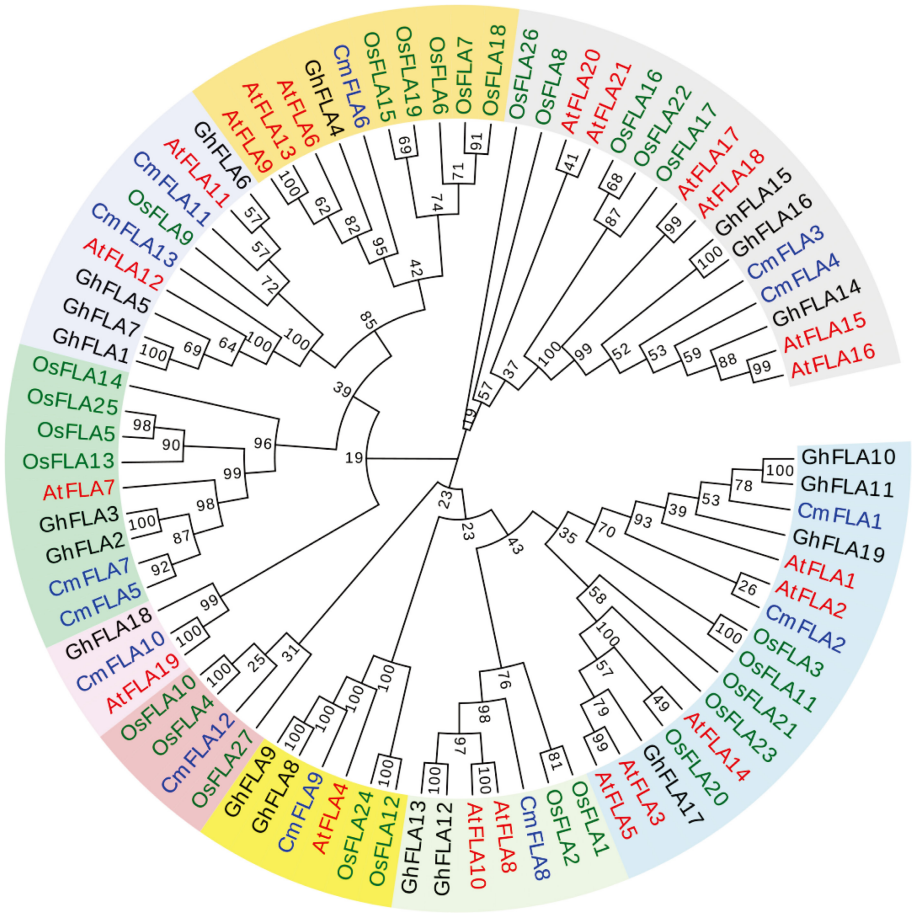

Fig. 3 Phylogenetic relationship of FLAs between melon and other species. Red color represents *Arabidopsis thaliana* (At); blue color represents *Cucumis melon* (Cm); green color represents *Oryza sativa* (Os); and black color represents *Gossypium hirsutum* (Gh). The phylogenetic tree was constructed using MEGA 7 software with the Neighbor-Joining method, employing a bootstrap value of 1,000 replicates. The GenBank accession numbers of the sequences were used for the analyses, as detailed in Supplementary Table S4.

demonstrated a positive correlation with fruit maturation, whereas the majority of *CmFLAs* exhibited a negative relationship (Fig. 4b).

GO analysis of CmFLAs

GO annotation is an effective tool for describing gene localizations and functions. Consequently, the GO annotations of CmFLAs were employed to describe biological processes, cellular components, and molecular functions were determined. The results of GO analysis indicated that CmFLAs were enriched in cellular components, integral components of membranes, membrane, and anchored components of plasma membrane of the cellular component categories (Supplementary Fig. S1, Supplementary Table S5). Within the molecular function categories, molecular function, gamma-glutamyltransferase activity, actin binding, and polysaccharide binding were found (Supplementary Fig. S1, Supplementary Table S5). Moreover, biological process, cell adhesion, and response to salt stress exhibited high enrichment (Supplementary Fig. S1, Supplementary Table S5). Additionally, the GO annotation analysis highlighted the involvement of CmFLA2, CmFLA9, and CmFLA12 in response to salt stress (Supplementary Table S5).

Cis-element analysis of CmFLAs promoter

Putative *cis*-elements in the promoter of *CmFLAs* were predicted using PlantCARE. It was observed that all *CmFLA* promoters contained light-responsive elements, with some also possessing circadian control elements. Additionally, the promoter regions exhibited an abundance of hormonal or environment-responsive elements, including ABA responsiveness, auxin-responsive element, gibberellin-responsiveness, salicylic acid responsiveness, defense and stress responsiveness, low-temperature responsiveness, and drought induction (Supplementary Fig. S2).

Furthermore, the promoter of *CmFLA6* and *CmFLA12* contained MYBHv1 binding site. Additionally, *CmFLA8* promoter contained a protein binding site, while a cis-acting regulatory element was found in the promoter of *CmFLA10* (Supplementary Fig. S2).

Expression analysis of *CmFLAs* in different melon cultivars

To investigate the relationship between the expression of *CmFLAs* and total soluble solids content (TSS), we examined the expression of *CmFLAs* in melon fruits from various melon cultivars (Fig. 5a). The qRT-PCR results indicated that the expression levels of *CmFLA1*, *3*, 6, *7*, *8*, *11*, and *13* in BLC, HPC, and BCG (low TSS cultivars) were higher compared to XM, YJ, LT4, GS, and M43 (high TSS cultivars). Correlation analysis between TSS and gene expression indicated most of the *CmFLAs* were negatively related to TSS (Fig. 5b).

ABA inhibited the expression of *CmFLA4*, *6*, and *11* in melon fruit

The promoter elements of CmFLA1, 3, 4, 5, and 8 suggest the potential involvement of these genes in ABA responsiveness (Supplementary Fig. S2). Subsequently, we examined the gene expression of *CmFLAs* after ABA treatment in melon fruit of high TSS cultivar. Our findings indicated that the expression of *CmFLA4*, *6*,

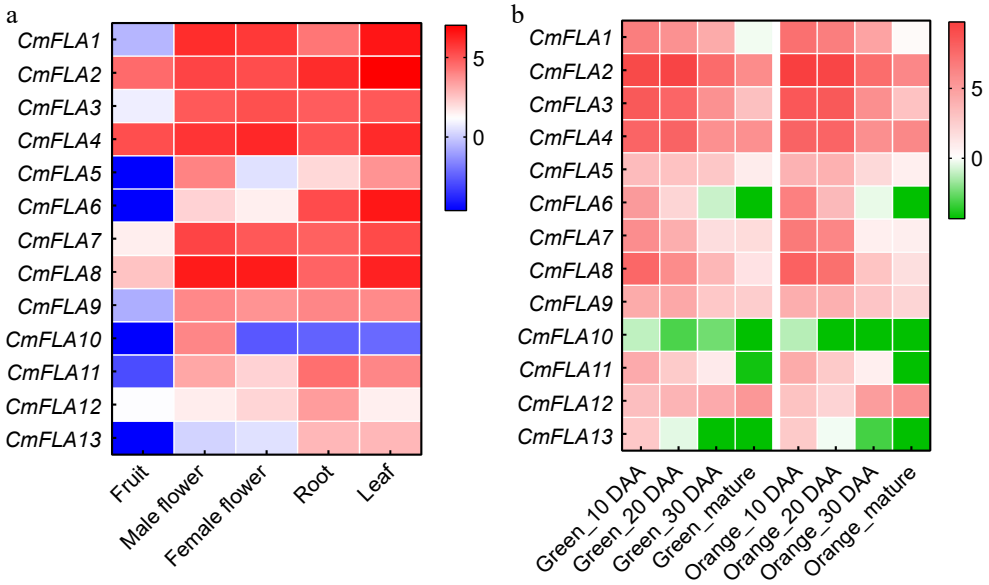

Fig. 4 Heatmaps show the expression analysis of *CmFLA* gene. (a) Expression profiles of *CmFLA* genes in different organs. Project: PRJNA383830. (b) Expression profiles of *CmFLAs* genes in fruit at different developmental stages. Expression was quantified on the indicated day after anthesis (DAA). Project: PRJNA286120. Scaled log2 expression values based on RNA-seq data are shown from blue to red, indicating low to high expression levels. The data were obtained from the Cucurbitgenomics database (http://cucurbitgenomics.org/rnaseq/home).

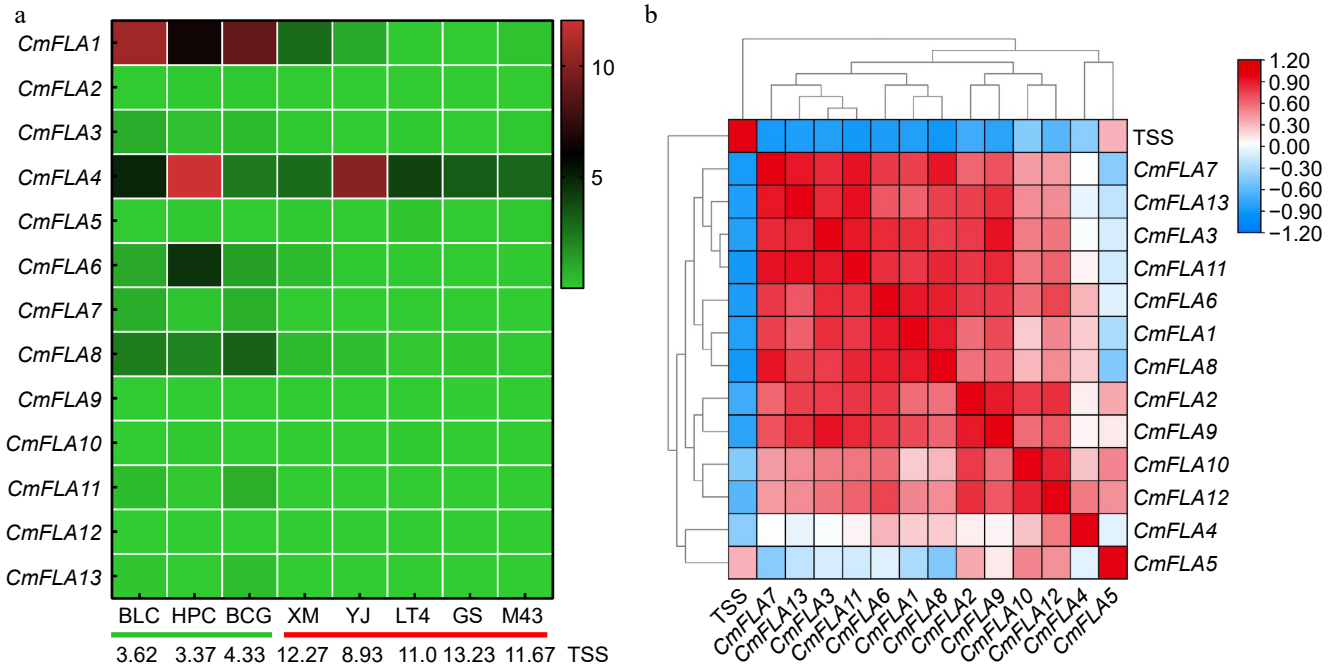

Fig. 5 Correlation analysis between total soluble solid contents (TSS) and gene expression of *CmFLAs*. (a) Heatmap of the *CmFLA* genes in melon fruit at 30 DAA from various cultivars obtained using qRT-PCR analysis. *TUA* (α-tubulin) was used as reference gene. Expression values based on qRT-PCR data are shown from green to red, indicating low to high expression. The values at the bottom of the figure indicate the TSS for each melon cultivars. The green line represents low TSS cultivars, and the red line represents high TSS cultivars. (b) TSS and gene expression correlation analysis in melon fruit at 30 DAA from various cultivars. Data are shown from blue to red, indicating low to high correlation.

and *11* was repressed by ABA, while the expression of other genes remained unaffected (Supplementary Fig. S3).

Sugar content increased after β-Glc Yariv treatment in melon fruit

β-Glc Yariv was sprayed on the melon fruit of the cv. 'BCG' (low TSS cultivars) at 20 DAA to investigate its effects on *CmFLAs* gene expression and sugar content. The results showed that the expression of *CmFLA1*, *8*, *11*, and *13* was suppressed after β-Glc Yariv treatment (Fig. 6a). The samples were further analyzed for sugar content by GC. The results revealed a significant increase in sucrose content in the β-Glc Yariv treated samples compared to the control, accompanied by a decrease in fructose content (Fig. 6b).

To identify genes associated with changes in sugar content, we performed an expression analysis of sugar metabolism-related genes. This analysis revealed a significant increase in the expression of alkaline a-galactosidase/neutral a-galactosidase genes (CmAAG1, CmAAG2; CmNAG1, CmNAG2, CmNAG3), which are associated with

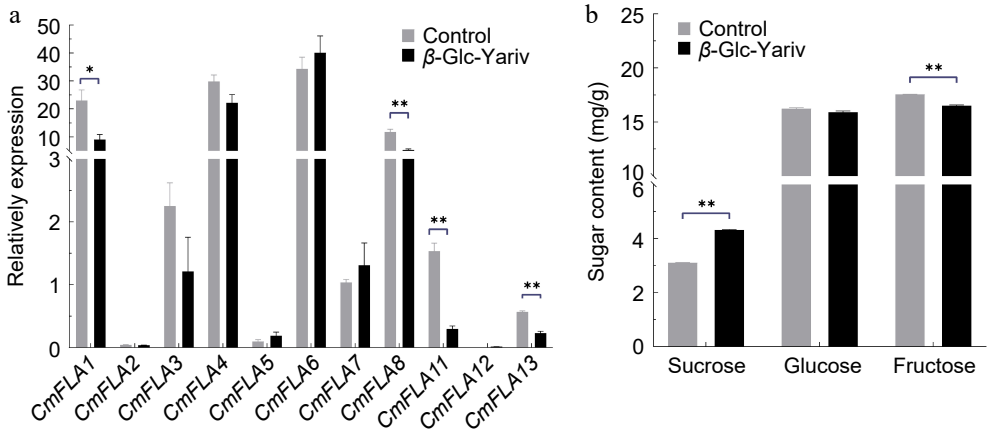

Fig. 6 Sugar content and gene expression of *CmFLAs* after *β*-Glc Yariv treatment in melon fruit. Melon fruits of the cv. 'BCG' at 20 DAA were sprayed with *β*-Glc Yariv solution. (a) Gene expression of *CmFLAs* after *β*-Glc Yariv treatment. *TUA* (*α*-tubulin) was used as reference gene. (b) Sugar content after *β*-Glc Yariv treatment. Water was used as the control. Data represent means of three biological replicates ± SE. Statistical significance was denoted as * $p < 0.05$, ** $p < 0.01$ by t-test.

the breakdown of RFOs into sucrose[50]. Similarly, the expression of neutral invertase genes (CmNIN1/3/4) was upregulated, while acid invertase gene *CmAIN2* was down-regulated, which is responsible for hydrolyzing sucrose into glucose and fructose[51]. Additionally, the expression of *CmSPS1* and *CmSPS2,* responsible for synthesizing UDP-glucose with fructose-6P into sucrose-P[52], was also increased. No significant difference was observed in the expression of *CmSUSs* genes compared to the control. Furthermore, the tonoplast sugar transporter CmTST2, known for promoting sugar accumulation in the vacuole[45], exhibited elevated expression after *β*-Glc Yariv treatment (Supplementary Fig. S4).

CmFLA8 localizes to the cytoplasm to inhibit glucose accumulation in melon fruit

We then investigated the function of the *CmFLA8* gene, which is highly expressed in melon fruit and significantly reduced following inhibitor treatment, to determine its role in regulating fruit sugar accumulation. Localization studies in tobacco protoplasts confirmed cytoplasmic expression of CmFLA8 (Fig. 7a). We then employed a melon transient expression system to validate the function of CmFLA8 in fruit (Fig. 7b). The expression of *CmFLA8* in overexpressing fruits (CmFLA8-OE) was significantly higher than that in the control fruits (Fig. 7c). Subsequent assessment of fruit sugar levels

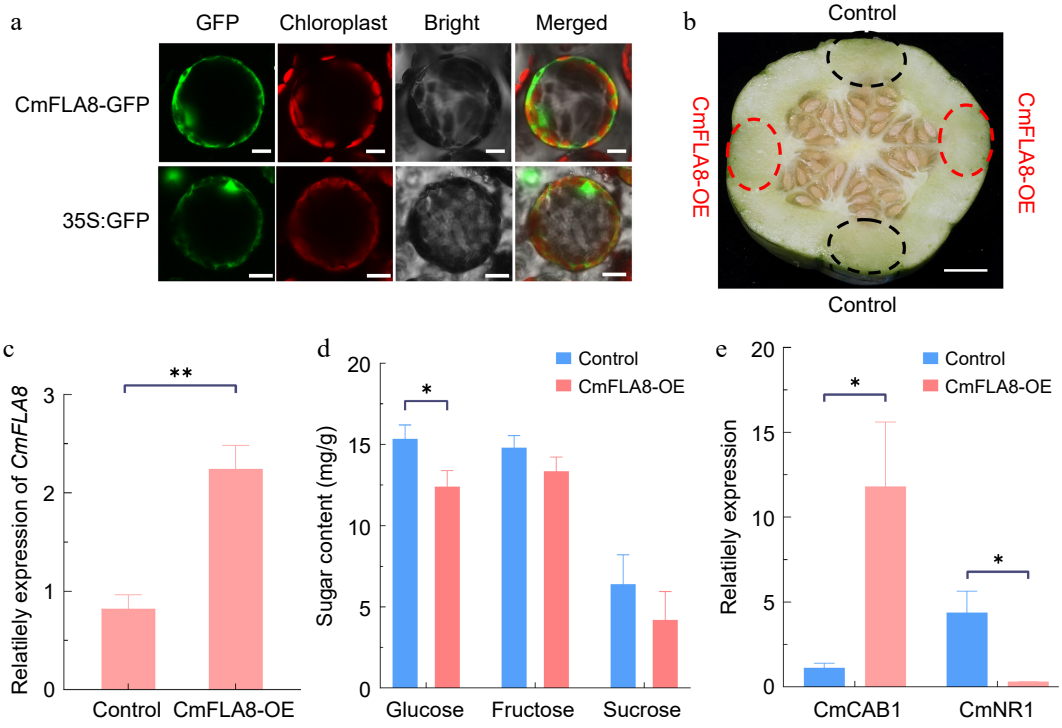

Fig. 7 Gene function verification of CmFLA8. (a) Subcellular localization of CmFLA8 in *N. benthamiana* protoplasts. Scale bars =10 μm. (b) Transient expression of CmFLA8-OE in melon fruit. CmFLA8-OE agrobacterium cells were injected into the melon tissue, with the pHELLSGATE8-HA vector used as a control. The dotted circles indicate the injection sites, scale bar = 1 cm. (c) Relative expression of *CmFLA8* in CmFLA8-OE melon fruit. Reference gene: Tubulin. (d) Sugar concentrations in CmFLA8-OE melon fruit. (e) qRT-PCR analysis of CAB1 and NR1 expression in melon fruit. Reference gene: Tubulin. Empty vector, control fruit expressed the empty pHELLSGATE8-HA vector. Data represent means of four replicates ± SE. * $p < 0.05$ and ** $p < 0.01$ by t-test.

revealed a notable decrease in glucose content in CmFLA8-OE compared to control fruit, as shown in Fig. 7d. In Arabidopsis, glucose represses *chlorophyllab-binding protein1* (CAB1) expression while inducing the *nitrate reductase1 gene* (*NR1*)[53]. Consequently, these genes serve as markers to signify alterations in cytoplasmic glucose levels. We identified melon homologs, CmCAB1 and CmNR1, showing high sequence similarity to these Arabidopsis proteins. Expression analysis revealed an increase in *CmCAB1* expression and a decrease in *CmNR1* expression in CmFLA8-OE fruits (Fig. 7e), indicating a decrease in glucose in the cytoplasm.

Discussion

Identification of melon FLAs

In this study, we identified 13 *CmFLAs* in melon and divided them into four groups (Fig. 2b). All CmFLAs recognized as secretory proteins with N-terminal signal peptides and FAS domains containing three highly conserved motifs (H1, H2, and YF), similar to other plant FLAs[10,11]. The GPI-anchor can be cleaved from the protein by endogenous GPI-specific phospholipases or other enzymes, releasing the protein into the extracellular space[54]. The GPI-modification signal is crucial for membrane anchoring, efficient ER exit, secretion, and plasma membrane localization of AtFLA4[12]. Thus, the GPI-anchor signal is vital for maintaining FLA function. Among the 13 CmFLAs identified, five possess the GPI-anchor signal; however, further experiments are needed to ascertain the precise role of the GPI-anchor signal.

Glycosylation involves the post-translational modification of Pro residues to Hyp, and the type of glycosylation relies on the presence of contiguous or noncontiguous Hyp residues[10]. Two types of glycosylation, *N*-glycosylation, and *O*-glycosylation, are observed in FLAs. *N*-glycosylation, occurring on Asn residues, is a characteristic feature, while *O*-glycosylation, involving the glycosylation of hydroxyl groups on the side chains of amino acids, is more complex[55]. The position of *N*-glycosylation site is predicted within the FAS domains of FLA[10,47]. *N*-glycosylation in AtFLA4 plays a vital role in ER-exit, whereas *O*-glycosylation influences post-secretory fate[12]. Additionally, the *O*-glycosylation of AtAGP21 is crucial for secretion and cellular targeting[56]. CmFLAs were predicted to contain 1–6 *N*-glycosylation sites. Furthermore, CmFLA6 and CmFLA13 were found to have fewer than 10 O-glycosylation sites, while the remaining CmFLAs contain 10–35 sites (Table 2), suggesting potential variations in their glycosylation patterns.

Melon FLAs were negatively correlated with fruit ripening and sugar accumulation

The expression of most *CmFLAs* is inversely associated with fruit ripening and TSS content (Figs 4b & 5), indicating a potential role for CmFLAs as negative regulators during melon fruit ripening. In tomato, several *SlFLA* genes were notably downregulated during fruit ripening stages, and silencing of *SlFLA13* accelerates tomato fruit ripening and enhances carotenoid accumulation[57].

In this study, some *CmFLAs,* such as *CmFLA1, 8, 11,* and *13*, exhibited a negative correlation between their expression and fruit ripening as well as sugar content (Figs 4b & 5). Treatment with β-Glc Yariv led to a reduction in their expression and an increase in sugar content (Fig. 6a). Expression analysis of sugar metabolism-related genes revealed an increase in *CmAAG/NAG*s after β-Glc Yariv treatment (Supplementary Fig. S4). In watermelon, ClAGA2 is a pivotal factor in controlling stachyose and raffinose hydrolysis, thereby influencing fruit sugar accumulation[50]. According to the model of sugar unloading and post-phloem transport in melon fruit, α-galactosidase represents an essential step in sucrose accumulation[50]. Elevated *CmAAG/NAG* expression promotes greater sucrose production. Notably, the expression levels of *CmNAGs* surpassed those of *CmAAGs* in Supplementary Fig. S4, suggesting the potential heightened importance of CmNAGs compared to CmAAGs in melon fruit.

Invertase enzymes are classified as CWINs, VINs, and CINs based on their cellular localization in the cell wall, vacuole, and cytosol. CINs are categorized as NINs, while CWINs and VINs are classified as AINs[51]. The vacuole can store high concentrations of sugars[58]. Upon sucrose entry into the fruit pulp cells or fruit parenchyma cells, CmAIN2 breaks it down into glucose and fructose. Consequently, reduced *CmAIN2* expression leads to a decrease in sucrose hydrolysis (Supplementary Fig. S4), resulting in a reduction in fructose content (Fig. 6b). Moreover, increased expression of *CmSPS1/2* gene in β-Glc Yariv treatment facilitated sucrose synthesis in the cytoplasm, with the resulting sugars promptly transported into the vacuole by CmTST2[45]. Consequently, sugar content increased after β-Glc Yariv treatment in melon fruit (Fig. 6b).

Our investigation confirmed that CmFLA8 is localized in the cytoplasm and inhibits glucose accumulation in melon fruit. Additionally, it influences fructose and sucrose levels; however, the observed effect was not statistically significant (Fig. 7). Thus, it is conceivable that CmFLA1, 11, and 13 could also impact sugar levels. Due to the lack of prior research on the impact of FLA proteins on sugar accumulation, we propose a potential role for FLA proteins in modulating sugar-metabolic enzymes or their upstream-regulated transcription factors through post-translational modifications. Further experiments are necessary to elucidate how these CmFLA protein specifically affect the sugar content in melon.

ABA-responsive element was identified in the promoter regions of *CmFLA4* (Supplementary Fig. S2). For *CmFLA4*, *6*, and *11*, their expression displayed a negative correlation with fruit ripening and was inhibited by ABA (Fig. 4b; Supplementary Fig. S3). ABA plays an important role in promoting the ripening of numerous fleshy fruits[59]. Additionally, the expression of certain FLA genes has been observed to be downregulated by ABA in other plant species[10,25,60]. Consequently, *CmFLA4, 6,* and *11* may influence the expression of sugar synthesis or sugar transporter-related genes during the early stages of fruit development, resulting in reduced sugar content in the fruit. As melon fruit matures, ABA signaling may suppress the expression of these genes, thereby facilitating the activation of sugar accumulation-related genes and promoting sugar accumulation. The expression of these *CmFLAs* may be under the regulation of ABA-signal transduction factors, further experiments are needed to verify this hypothesis.

Conclusions

In conclusion, 13 CmFLAs were identified in the melon genome and were clustered into four groups based on FAS motifs and AGP-regions. The comprehensive structural, phylogenetic, chromosomal localization, expression analyses, and promoter prediction in this study shed light on the functions of FLAs in melon. *CmFLA10* and *CmFLA12* exhibited tissue-specific expression patterns. Furthermore, expression analysis revealed a negative correlation between most *CmFLAs* and fruit ripening as well as TSS accumulation. When melon fruit was treated with β-Glc Yariv, the expression of *CmFLA1*, *8*, *11*, and *13* was downregulated. Concurrently, the transcript levels of sugar metabolism-related genes and sugar transporters were upregulated. Consequently, sucrose accumulation was enhanced while the fructose content in the vacuoles was diminished. CmFLA8 is localized in the cytoplasm. Moreover, the transient overexpression of CmFLA8 in melon fruits resulted in a reduction in glucose content compared to the control. Further research, such as the use of CRISPR

technology for gene knockout or transgenic technology for overexpression, is necessary to elucidate the function of specific functions of individual FLA genes. Overall, these findings may provide valuable insights for future investigations into the biological function of FLAs in melon.

Author contributions

The authors confirm contribution to the paper as follows: study conception and design, experiment conducting, data analysis, manuscript writing: Wen S; data collection: Sun R, Gao M; analysis and interpretation of results: Huang R, Li J, Zhou Y; research supporting, manuscript revision: Cheng J; critical feedback providing and research revision: Bie Z. All authors reviewed the results and approved the final version of the manuscript.

Data availability

The datasets generated during and/or analyzed during the current study are available from the corresponding author on reasonable request.

Acknowledgments

This work was supported by the Hubei Provincial Funding Programme to Support High-Quality Development of the Seed Industry (HBZY2023B004-5) to Jintao Cheng, and the China Postdoctoral Science Foundation (2022M711276) to Suying Wen.

Conflict of interest

The authors declare that they have no conflict of interest.

Supplementary information accompanies this paper at (https://www.maxapress.com/article/doi/10.48130/vegres-0025-0004)

Dates

Received 11 December 2024; Revised 13 January 2025; Accepted 3 February 2025; Published online 27 March 2025

References

1. Showalter AM, Keppler BD, Lichtenberg J, Gu D, Welch LR. 2010. A bioinformatics approach to the identification, classification, and analysis of hydroxyproline-rich glycoproteins. *Plant Physiology* 153:485–513
2. Johnson KL, Cassin AM, Lonsdale A, Wong GKS, Soltis DE, et al. 2017. Insights into the evolution of hydroxyproline-rich glycoproteins from 1000 plant transcriptomes. *Plant Physiology* 174:904–21
3. Ellis M, Egelund J, Schultz CJ, Bacic A. 2010. Arabinogalactan-proteins: key regulators at the cell surface? *Plant Physiology* 153:403–19
4. Huang G, Gong S, Xu W, Li W, Li P, et al. 2013. A fasciclin-like arabinogalactan protein, GhFLA1, is involved in fiber initiation and elongation of cotton. *Plant Physiology* 161:1278–90
5. Kitazawa K, Tryfona T, Yoshimi Y, Hayashi Y, Kawauchi S, et al. 2013. β-galactosyl Yariv reagent binds to the β-1,3-galactan of arabinogalactan proteins. *Plant Physiology* 161:1117–26
6. Leszczuk A, Szczuka E, Wydrych J, Zdunek A. 2018. Changes in arabinogalactan proteins (AGPs) distribution in apple (*Malus* x *domestica*) fruit during senescence. *Postharvest Biology and Technology* 138:99–106
7. Leszczuk A, Kalaitzis P, Blazakis KN, Zdunek A. 2020. The role of arabinogalactan proteins (AGPs) in fruit ripening-a review. *Horticulture Research* 7:176
8. Huber O, Sumper M. 1994. Algal-CAMs: isoforms of a cell adhesion molecule in embryos of the alga volvox with homology to Drosophila fasciclin I. *The EMBO Journal* 13:4212–22
9. Kim JE, Jeong HW, Nam JO, Lee BH, Choi JY, et al. 2002. Identification of motifs in the fasciclin domains of the transforming growth factor-β-induced matrix protein βig-h3 that interact with the $\alpha v\beta 5$ integrin. *Journal of Biological Chemistry* 277:46159–65
10. Johnson KL, Jones BJ, Bacic A, Schultz CJ. 2003. The fasciclin-like arabinogalactan proteins of Arabidopsis. A multigene family of putative cell adhesion molecules. *Plant Physiology* 133:1911–25
11. Faik A, Abouzouhair J, Sarhan F. 2006. Putative fasciclin-like arabinogalactan-proteins (FLA) in wheat (*Triticum aestivum*) and rice (*Oryza sativa*): identification and bioinformatic analyses. *Molecular Genetics and Genomics* 276:478–94
12. Xue H, Veit C, Abas L, Tryfona T, Maresch D, et al. 2017. *Arabidopsis thaliana FLA4* functions as a glycan-stabilized soluble factor via its carboxy-proximal Fasciclin 1 domain. *The Plant Journal* 91:613–30
13. Ma H, Zhao J. 2010. Genome-wide identification, classification, and expression analysis of the arabinogalactan protein gene family in rice (*Oryza sativa* L.). *Journal of Experimental Botany* 61:2647–68
14. Huang G, Xu W, Gong S, Li B, Wang X, et al. 2008. Characterization of 19 novel cotton *FLA* genes and their expression profiling in fiber development and in response to phytohormones and salt stress. *Physiologia Plantarum* 134:348–59
15. Wang H, Jiang C, Wang C, Yang Y, Yang L, et al. 2015. Antisense expression of the fasciclin-like arabinogalactan protein *FLA6* gene in *Populus* inhibits expression of its homologous genes and alters stem biomechanics and cell-wall composition in transgenic trees. *Journal of Experimental Botany* 66:1291–302
16. Liu H, Shi R, Wang X, Pan Y, Li Z, et al. 2013. Characterization and expression analysis of a fiber differentially expressed Fasciclin-like arabinogalactan protein gene in Sea Island cotton fibers. *PLoS One* 8:e70185
17. Guerriero G, Mangeot-Peter L, Legay S, Behr M, Lutts S, et al. 2017. Identification of fasciclin-like arabinogalactan proteins in textile hemp (*Cannabis sativa* L.): *in silico* analyses and gene expression patterns in different tissues. *BMC Genomics* 18:741
18. Li J, Yu M, Geng L, Zhao J. 2010. The fasciclin-like arabinogalactan protein gene, *FLA3*, is involved in microspore development of Arabidopsis. *The Plant Journal* 64:482–97
19. Tan H, Liang W, Hu J, Zhang D. 2012. MTR1 encodes a secretory fasciclin glycoprotein required for male reproductive development in rice. *Developmental Cell* 22:1127–37
20. Deng Y, Wan Y, Liu W, Zhang L, Zhou K, et al. 2022. *OsFLA1* encodes a fasciclin-like arabinogalactan protein and affects pollen exine development in rice. *Theoretical and Applied Genetics* 135:1247–62
21. Showalter AM, Keppler BD, Liu X, Lichtenberg J, Welch LR. 2016. Bioinformatic identification and analysis of hydroxyproline-rich glycoproteins in *Populus trichocarpa*. *BMC Plant Biology* 16:229
22. Takahashi D, Kawamura Y, Uemura M. 2016. Cold acclimation is accompanied by complex responses of glycosylphosphatidylinositol (GPI)-anchored proteins in Arabidopsis. *Journal of Experimental Botany* 67:5203–15
23. Cagnola JI, Dumont de Chassart GJ, Ibarra SE, Chimenti C, Ricardi MM, et al. 2018. Reduced expression of selected *FASCICLIN-LIKE ARABINOGALACTAN PROTEIN* genes associates with the abortion of kernels in field crops of *Zea mays* (maize) and of Arabidopsis seeds. *Plant, Cell & Environment* 41:661–74
24. Ma Y, MacMillan CP, de Vries L, Mansfield SD, Hao P, et al. 2022. FLA11 and FLA12 glycoproteins fine-tune stem secondary wall properties in response to mechanical stresses. *New Phytologist* 233:1750–67
25. Allelign Ashagre H, Zaltzman D, Idan-Molakandov A, Romano H, Tzfadia O, et al. 2021. FASCICLIN-LIKE 18 is a new player regulating root elongation in *Arabidopsis thaliana*. *Frontiers in Plant Science* 12:645286
26. Liu E, MacMillan CP, Shafee T, Ma Y, Ratcliffe J, et al. 2020. Fasciclin-like arabinogalactan-protein 16 (FLA16) is required for stem development in *Arabidopsis*. *Frontiers in Plant Science* 11:615392
27. Macmillan CP, Mansfield SD, Stachurski ZH, Evans R, Southerton SG. 2010. Fasciclin-like arabinogalactan proteins: specialization for stem biomechanics and cell wall architecture in Arabidopsis and *Eucalyptus*. *The Plant Journal* 62:689–703
28. Miao Y, Cao J, Huang L, Yu Y, Lin S. 2021. *FLA14* is required for pollen development and preventing premature pollen germination under high humidity in Arabidopsis. *BMC Plant Biology* 21:254

29. Shi H, Kim Y, Guo Y, Stevenson B, Zhu J. 2003. The Arabidopsis *SOS5* locus encodes a putative cell surface adhesion protein and is required for normal cell expansion. *The Plant Cell* 15:19–32
30. Xu S, Rahman A, Baskin TI, Kieber JJ. 2008. Two leucine-rich repeat receptor kinases mediate signaling, linking cell wall biosynthesis and ACC synthase in *Arabidopsis*. *The Plant Cell* 20:3065–79
31. Grumet R, Garcia-Mas J, Katzir N. 2017. Cucurbit genetics and genomics: a look to the future. In *Genetics and Genomics of Cucurbitaceae*, eds Grumet R, Katzir N, Garcia-Mas J. Cham: Springer. Volume 20. pp. 409–15. doi: 10.1007/7397_2017_1
32. Almagro Armenteros JJ, Tsirigos KD, Sønderby CK, Petersen TN, Winther O, et al. 2019. SignalP 5.0 improves signal peptide predictions using deep neural networks. *Nature Biotechnology* 37:420–23
33. Eisenhaber B, Bork P, Eisenhaber F. 1999. Prediction of potential GPI-modification sites in proprotein sequences. *Journal of Molecular Biology* 292:741–58
34. Wilkins MR, Gasteiger E, Bairoch A, Sanchez JC, Williams KL, et al. 1999. Protein identification and analysis tools in the ExPASy server. In *2-D Proteome Analysis Protocols*, ed. Link AJ. US: Humana Press. Volume 112. pp. 531–52. doi: 10.1385/1-59259-584-7:531
35. Horton P, Park KJ, Obayashi T, Fujita N, Harada H, et al. 2007. WoLF PSORT: protein localization predictor. *Nucleic Acids Research* 35:W585–W587
36. Gupta R, Brunak S. 2002. Prediction of glycosylation across the human proteome and the correlation to protein function. *Biocomputing 2002* 2001:310–22
37. Steentoft C, Vakhrushev SY, Joshi HJ, Kong Y, Vester-Christensen MB, et al. 2013. Precision mapping of the human O-GalNAc glycoproteome through SimpleCell technology. *The EMBO Journal* 32:1478–88
38. Chen C, Chen H, Zhang Y, Thomas HR, Frank MH, et al. 2020. TBtools: an integrative toolkit developed for interactive analyses of big biological data. *Molecular Plant* 13:1194–1202
39. Wang J, Chitsaz F, Derbyshire MK, Gonzales NR, Gwadz M, et al. 2023. The conserved domain database in 2023. *Nucleic Acids Research* 51:D384–D388
40. Bailey TL, Boden M, Buske FA, Frith M, Grant CE, et al. 2009. MEME SUITE: tools for motif discovery and searching. *Nucleic Acids Research* 37:W202–W208
41. Larkin MA, Blackshields G, Brown NP, Chenna R, McGettigan PA, et al. 2007. Clustal W and clustal X version 2.0. *Bioinformatics* 23:2947–48
42. Kumar S, Stecher G, Tamura K. 2016. MEGA7: molecular evolutionary genetics analysis version 7.0 for bigger datasets. *Molecular Biology and Evolution* 33:1870–74
43. He Z, Zhang H, Gao S, Lercher MJ, Chen WH, et al. 2016. Evolview v2: an online visualization and management tool for customized and annotated phylogenetic trees. *Nucleic Acids Research* 44:W236–W241
44. Lescot M, Déhais P, Thijs G, Marchal K, Moreau Y, et al. 2002. PlantCARE, a database of plant *cis*-acting regulatory elements and a portal to tools for *in silico* analysis of promoter sequences. *Nucleic Acids Research* 30:325–27
45. Cheng J, Wen S, Xiao S, Lu B, Ma M, et al. 2018. Overexpression of the tonoplast sugar transporter CmTST2 in melon fruit increases sugar accumulation. *Journal of Experimental Botany* 69:511–23
46. Livak KJ, Schmittgen TD. 2001. Analysis of relative gene expression data using real-time quantitative PCR and the $2^{-\Delta\Delta CT}$ method. *Methods* 25:402–8
47. Schultz CJ, Rumsewicz MP, Johnson KL, Jones BJ, Gaspar YM, et al. 2002. Using genomic resources to guide research directions. The arabinogalactan protein gene family as a test case. *Plant Physiology* 129:1448–63
48. Shpak E, Barbar E, Leykam JF, Kieliszewski MJ. 2001. Contiguous hydroxyproline residues direct hydroxyproline arabinosylation in *Nicotiana tabacum*. *Journal of Biological Chemistry* 276:11272–78
49. Tan L, Leykam JF, Kieliszewski MJ. 2003. Glycosylation motifs that direct arabinogalactan addition to arabinogalactan-proteins. *Plant Physiology* 132:1362–69
50. Ren Y, Li M, Guo S, Sun H, Zhao J, et al. 2021. Evolutionary gain of oligosaccharide hydrolysis and sugar transport enhanced carbohydrate partitioning in sweet watermelon fruits. *The Plant Cell* 33:1554–73
51. Wan H, Wu L, Yang Y, Zhou G, Ruan YL. 2018. Evolution of sucrose metabolism: the dichotomy of invertases and beyond. *Trends in Plant Science* 23:163–77
52. Dai N, Cohen S, Portnoy V, Tzuri G, Harel-Beja R, et al. 2011. Metabolism of soluble sugars in developing melon fruit: a global transcriptional view of the metabolic transition to sucrose accumulation. *Plant Molecular Biology* 76:1–18
53. Wingenter K, Schulz A, Wormit A, Wic S, Trentmann O, et al. 2010. Increased activity of the vacuolar monosaccharide transporter TMT1 alters cellular sugar partitioning, sugar signaling, and seed yield in Arabidopsis. *Plant Physiology* 154:665–77
54. Fujihara Y, Ikawa M. 2016. GPI-AP release in cellular, developmental, and reproductive biology. *Journal of Lipid Research* 57:538–45
55. Liang R, You L, Dong F, Zhao X, Zhao J. 2020. Identification of hydroxyproline-containing proteins and hydroxylation of proline residues in rice. *Frontiers in Plant Science* 11:1207
56. Borassi C, Gloazzo Dorosz J, Ricardi MM, Carignani Sardoy M, Pol Fachin L, et al. 2020. A cell surface arabinogalactan-peptide influences root hair cell fate. *New Phytologist* 227:732–43
57. Hu J, Wang J, Muhammad T, Tuerdiyusufu D, Yang T, et al. 2024. Functional analysis of fasciclin-like arabinogalactan in carotenoid synthesis during tomato fruit ripening. *Plant Physiology and Biochemistry* 210:108589
58. Jung B, Ludewig F, Schulz A, Meißner G, Wöstefeld N, et al. 2015. Identification of the transporter responsible for sucrose accumulation in sugar beet taproots. *Nature Plants* 1:14001
59. Fenn MA, Giovannoni JJ. 2021. Phytohormones in fruit development and maturation. *The Plant Journal* 105:446–58
60. Seifert GJ, Xue H, Acet T. 2014. The *Arabidopsis thaliana FASCICLIN LIKE ARABINOGALACTAN PROTEIN 4* gene acts synergistically with abscisic acid signalling to control root growth. *Annals of Botany* 114:1125–33